JOURNAL OF THE AMERICAN CHEMICAL SOCIETY

Subscriber access provided by UNSW Library

Article

Daisy Chain Dendrimers: Integrated Mechanically Interlocked Molecules with Stimuli-induced Dimension Modulation Feature

Wei-Jian Li, Wei Wang, Xu-Qing Wang, Mu Li, Yubin Ke, Rui Yao, Jin Wen,
Guang-Qiang Yin, Bo Jiang, Xiaopeng Li, Panchao Yin, and Hai-Bo Yang

J. Am. Chem. Soc., **Just Accepted Manuscript** • DOI: 10.1021/jacs.0c02475 • Publication Date (Web): 17 Apr 2020

Downloaded from pubs.acs.org on April 17, 2020

Just Accepted

“Just Accepted” manuscripts have been peer-reviewed and accepted for publication. They are posted online prior to technical editing, formatting for publication and author proofing. The American Chemical Society provides “Just Accepted” as a service to the research community to expedite the dissemination of scientific material as soon as possible after acceptance. “Just Accepted” manuscripts appear in full in PDF format accompanied by an HTML abstract. “Just Accepted” manuscripts have been fully peer reviewed, but should not be considered the official version of record. They are citable by the Digital Object Identifier (DOI®). “Just Accepted” is an optional service offered to authors. Therefore, the “Just Accepted” Web site may not include all articles that will be published in the journal. After a manuscript is technically edited and formatted, it will be removed from the “Just Accepted” Web site and published as an ASAP article. Note that technical editing may introduce minor changes to the manuscript text and/or graphics which could affect content, and all legal disclaimers and ethical guidelines that apply to the journal pertain. ACS cannot be held responsible for errors or consequences arising from the use of information contained in these “Just Accepted” manuscripts.

is published by the American Chemical Society. 1155 Sixteenth Street N.W., Washington, DC 20036

Published by American Chemical Society. Copyright © American Chemical Society. However, no copyright claim is made to original U.S. Government works, or works produced by employees of any Commonwealth realm Crown government in the course of their duties.

Daisy Chain Dendrimers: Integrated Mechanically Interlocked Molecules with Stimuli-induced Dimension Modulation Feature

Wei-Jian Li[†], Wei Wang[†,*], Xu-Qing Wang[†], Mu Li[§], Yubin Ke[‡], Rui Yao[†], Jin Wen[^,*], Guang-Qiang Yin[†, #], Bo Jiang[†], Xiaopeng Li[#], Panchao Yin[§], Hai-Bo Yang[†,*]

[†]Shanghai Key Laboratory of Green Chemistry and Chemical Processes & Chang-Kung Chuang Institute, School of Chemistry and Molecular Engineering, East China Normal University, 3663 N. Zhongshan Road, Shanghai 200062, P. R. China.

[§]South China Advanced Institute for Soft Matter Science and Technology & State Key Laboratory of Luminescent Materials and Devices, South China University of Technology, Guangzhou, 510640 P. R. China.

[‡]Spallation Neutron Source Science Center, Dongguan 523803, China

[^]Institute of Theoretical Chemistry, Faculty of Vienna, University of Vienna, Währinger Str. 17, A-1090 Vienna, Austria

[#]Department of Chemistry, University of South Florida, Tampa, Florida 33620, United States.

ABSTRACT: The precise construction of the high-order mechanically interlocked molecules (MIMs) with well-defined topological arrangements of multiple mechanically interlocked units has been a great challenge. Herein, we present the first successful preparation of a new family of daisy chain dendrimers, in which the individual [c2]daisy chain rotaxane units serve as the branches of dendrimer skeleton. In particular, the third generation daisy chain dendrimer with twenty-one [c2]daisy chain rotaxane moieties was realized, which might be among the most complicated discrete high-order MIMs comprised of multiple [c2]daisy chain rotaxane units. Interestingly, such unique topological arrangements of multiple stimuli-responsive [c2]daisy chain rotaxanes endowed the resultant daisy chain dendrimers controllable and reversible nanoscale dimension modulation through the collective and amplified extension/contraction of each [c2]daisy chain rotaxane branch upon the addition of acetate anions or DMSO molecules as external stimulus. Furthermore, based on such intriguing size switching feature of daisy chain dendrimers, dynamic composite polymer films were constructed through the incorporation of daisy chain dendrimers into polymer films, which could undergo fast, reversible and controllable shape transformations when DMSO molecules were employed as stimulus. The successful merging of [c2]daisy chain rotaxanes and dendrimers described herein provides not only a brand-new type of high-order mechanically interlocked systems with well-defined topological arrangements of [c2]daisy chain rotaxanes, but also a successful and practical approach towards the construction of supramolecular dynamic materials.

INTRODUCTION

During the past few decades, mechanically interlocked molecules (MIMs) have evolved to be one of the most attractive fields within supramolecular chemistry and materials science because of their impressive topologies, structural beauty and unique dynamic features.[1] For instance, MIMs have proven to be a versatile platform for the construction of diverse artificial molecular machines[2] such as molecular shuttles,[3] molecular assemblers,[4] molecular pumps[5] and others[6] towards mimicking various biomolecular machines like kinesin, RNA polymerases, and ATP synthase.[7] Notably, among the numerous MIMs, [c2]daisy chain rotaxanes,[8] especially the bistable ones, have attracted increasing attention due to the direct and remarkable length changes of their backbones as well as the forces generated along with the molecular motions under various external stimuli. Such controllable motion behaviors at molecular scale have made them ideal candidates to act as “molecular muscles” that can mimic the sliding motions of actin and myosin filaments in sarcomeres.[9] Since the pioneering work by Sauvage and coworkers in 2000,[10] a great number of bistable [c2]daisy chain rotaxanes have been constructed as molecular muscles with various actuation mechanisms such as transition metal ion exchange, light irradiation, pH change, and solvent polarity switching.[11] Furthermore, inspired by the coordinative and amplified movements of sarcomeres that lead to the macroscopic motion of muscles,[12] many high-order (supramolecular) polymer systems with either linear or random arrangements of [c2]daisy chain rotaxanes have been successfully constructed through one-dimensional (1-D) covalent polymerization[13] and supramolecular polymerization[14] or three-dimensional (3-D) cross-linking polymerization.[15] These polymers can successfully convert the collective nanoscale motions of [c2]daisy chain rotaxanes to macroscopic muscle-like actuators. Although great achievements have been obtained in the field of (supramolecular) polymers based on [c2]daisy chain rotaxanes as key components, the construction of high-order discrete MIMs with both precise arrangements of multiple [c2]daisy chain rotaxanes and well-defined topological structures has been rarely explored possibly due to the lack of suitable and efficient synthetic approaches. Notably, the well-defined topological arrangements of [c2]daisy chain rotaxanes would offer great possibilities for the controllable, tunable or even programmable multidimensional actuations of the resultant integrated systems, thus imparting them potentially attractive switching features for the construction of stimuli-responsive supramolecular systems as well as dynamic materials.[16]

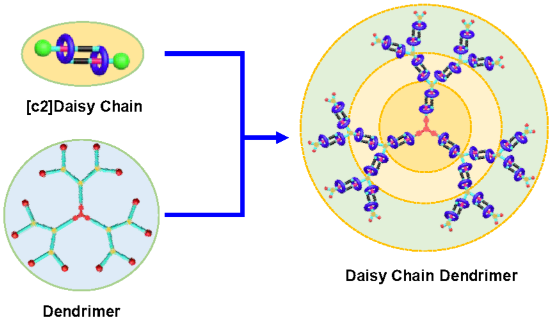

Figure 1. Schematic representation of a daisy chain dendrimer with [c2]daisy chain rotaxanes incorporated on the branches.

Considering the fact that dendrimers usually feature the star-shaped structures, highly branched topology and the nanometer-scale dimensions,[17] we envisioned that dendrimer might serve as a privileged platform for the precise arrangements of [c2]daisy chain rotaxanes, thus allowing for the well-defined monodispersed distributions of [c2]daisy chain rotaxanes within the dendrimer skeleton. In the proposed structure of daisy chain dendrimers as shown in Figure 1, the [c2]daisy chain rotaxanes serve as the branches of the dendrimers. We hypothesized that, due to the co-existence of multiple [c2]daisy chain rotaxanes with the precise topological arrangements, the controllable dimension modulation of the integrated daisy chain dendrimers would be feasible through the collective and amplified extension-contraction motions of [c2]daisy chain rotaxane branches. Moreover, on the basis of such unique size switching feature, the resultant daisy chain dendrimers could be further employed for the construction of novel supramolecular dynamic materials.

Herein, through the facile and efficient controllable divergent strategy, we realized the first successful and precise synthesis of the proposed daisy chain dendrimers up to the third generation. It should be noted that, in the resultant third-generation daisy chain dendrimer, twenty-one individual [c2]daisy chain rotaxane moieties monodispersedly distributed within the dendrimer skeleton, which might be among the most complicated discrete multiple [c2]daisy chain rotaxane systems with precise topological arrangements. As expected, through the collective and amplified muscle-like motions of individual [c2]daisy chain rotaxane branches upon the external stimuli, controllable and reversible stimuli-induced dimension modulation of the resultant daisy chain dendrimers was successfully realized in solution. In particular, the incorporation of daisy chain dendrimers into polymer films resulted in the successful construction of novel dynamic composite films, which featured intriguing solvent-induced shape transformations behavior in a controllable manner, thus making them promising candidates towards the construction of soft robotics.

RESULTS AND DISCUSSION

Preparation and characterization of daisy chain dendrimers up to the third generation. According to the retrosynthetic analysis, in order to realize the synthesis of the high-generation daisy chain dendrimers with stimuli-responsive dimension modulation feature, a new [c2]daisy chain rotaxane **1** (Figure 2a) with both reactive sites for dendrimer growth and stimuli-responsive sites for motion control was designed.

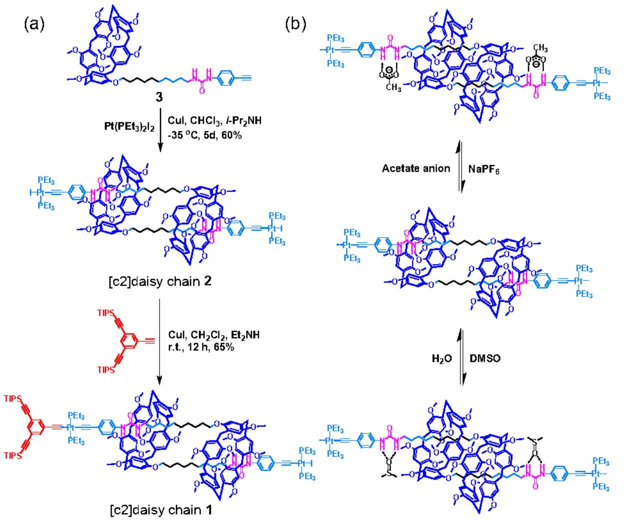

Figure 2. (a) Synthesis of [c2]daisy chain rotaxane **1** as the key precursor for the construction of daisy chain dendrimers (b) Proposed dual stimuli-induced reversible and controllable switching motion of the [c2]daisy chain rotaxane unit.

In this [c2]daisy chain rotaxane, mono-substituted platinum-acetylide moiety and two protected alkynes units were attached to the tails of the central [c2]daisy chain rotaxane core as both stoppers and dendrimer growth sites. In addition, on the basis of the host-guest property of pillar[5]arene (P[5]A),[18] both urea and alkyl chain unit were employed as the binding sites. Initially, due to the stronger N-H···O hydrogen-bond interactions between the urea moiety and methoxy group of P[5]A macrocycle compared to the CH···π interactions between neutral alkyl chain and P[5]A macrocycle, the P[5]A macrocycle preferred to encapsulating the urea moiety and the adjacent methylene units (*contracted state)*. Upon the addition of polar solvent molecule such as DMSO or anion such as acetate as stimulus, these hydrogen-bonding acceptors might interact with the urea moiety to "*push*" the P[5]A macrocycle to undergo translational motion towards the alkyl chain station, resulting in the direct length increase of the [c2]daisy chain rotaxane building block (*stretched state*) (Figure 2b). More importantly, through the addition and removal of the

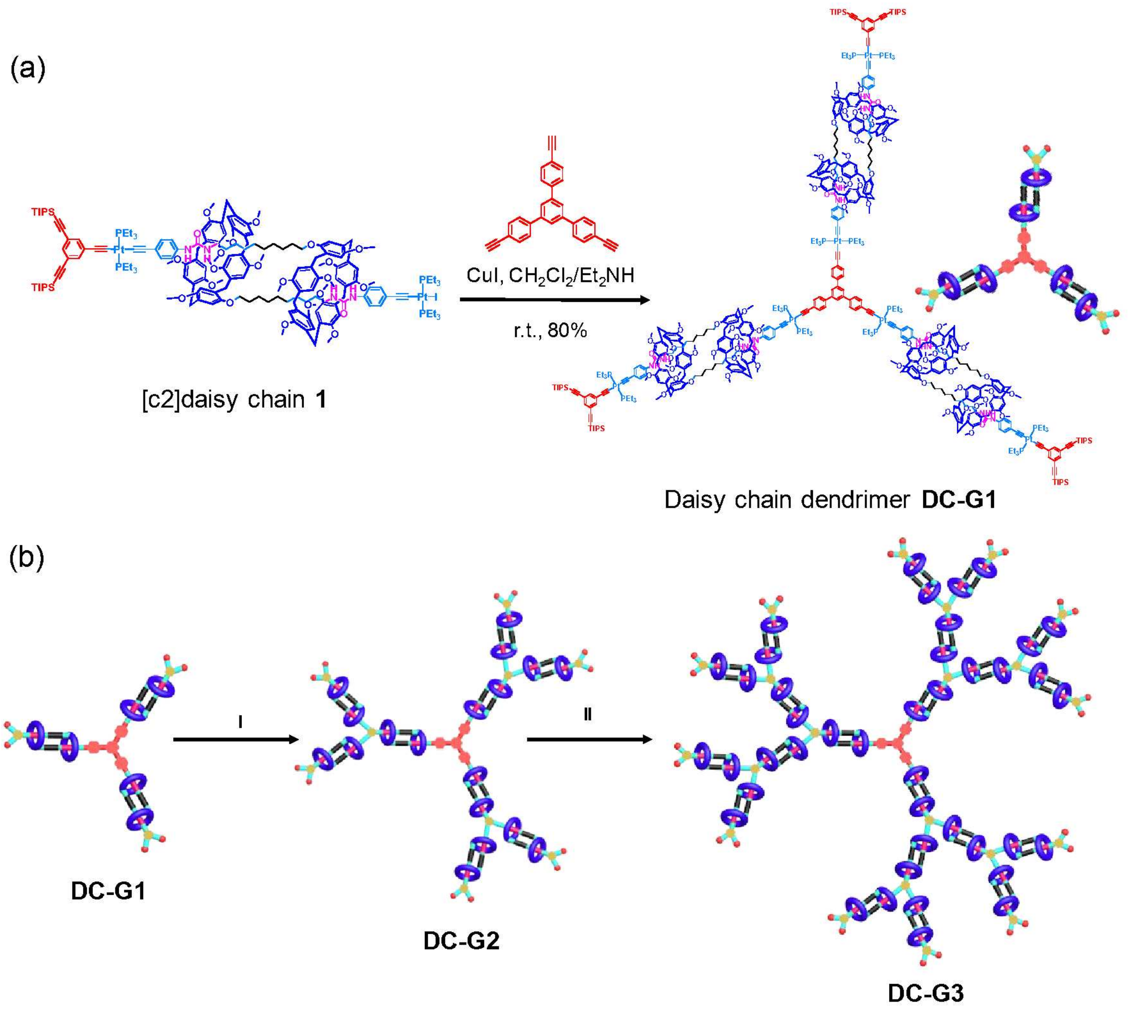

Figure 3. (a) Synthesis of daisy chain dendrimer **DC-G1**. (b) Schematic representation of a controllable divergent strategy for the synthesis of daisy chain dendrimers **DC-G2** and **DC-G3**. Reaction conditions: (I) (a) $Bu_4NF{\cdot}3H_2O$, THF, rt, 4 h, 76%; (b) **1**, CuI, DCM/Et_2NH, rt, 12 h, 84%; (II) (a) $Bu_4NF{\cdot}3H_2O$, THF, rt, 4 h, 81%; (b) **1**, CuI, DCM/Et_2NH, rt, 12 h, 65%.

external stimulus, reversible transformation between these two states of **1** could be realized, making **1** a bistable [c2]daisy chain rotaxane, thus laying the foundation for the 3-D dimension modulation of the integrated daisy chain dendrimers.

Following such design strategy, first of all, using the threading-followed-by-stoppering strategy and starting from compound **3** containing both the host (P[5]A) and guest (urea and alkyl chain) moieties, the employment of CuI-catalyzed coupling reaction between the terminal alkyne group and $Pt(PEt_3)_2I_2$ as the stoppering reaction at the optimized concentration (64 mM) led to the successful synthesis of a symmetrical [c2]daisy chain rotaxane precursor **2** in a relatively high yield (60%). Sequentially, by controlling the stoichiometric ratio of **2** and mono-alkyne compound, the selective coupling reaction of the mono-substituted platinum-acetylide moieties on one tail of **2** resulted in the successful synthesis of **1** as the key building block (Figure 2), which was fully characterized by 1-D multinuclear (^{1}H, ^{13}C, and ^{31}P), 2-D NMR (^{1}H-^{1}H COSY, ROESY) spectroscopy, and matrix-assisted laser desorption/ionization-time of flight mass spectrometry (MALDI-TOF-MS) analysis (Figures S2-S18).

With **1** as the key precursor in hand, a controllable divergent strategy was employed for the synthesis of the targeted daisy chain dendrimers incorporating individual [c2]daisy chain rotaxane unit on each branch as outlined in Figure 3. Taking advantage of the formation of platinum-acetylide bonds as the key growth step,[19] the first generation daisy chain dendrimer **DC-G1** with three switchable [c2]daisy chain rotaxane units was successfully prepared by the reaction of **1** and the core module 1,3,5-tris(4-ethynylphenyl)benzene in a good yield of 80%, at the outer periphery of which six protected alkynes co-existed. The sequential deprotection of these alkynes using tetrabutylammonium fluoride trihydrate ($Bu_4NF{\cdot}3H_2O$) afforded the formation of the corresponding intermediate **DC-G1-YNE** bearing six acetylene groups in 76% yield. Furthermore, repeating the coupling reaction of **DC-G1-YNE** and **1** generated the second-generation daisy chain dendrimer **DC-G2** with nine [c2]daisy chain rotaxane units and twelve

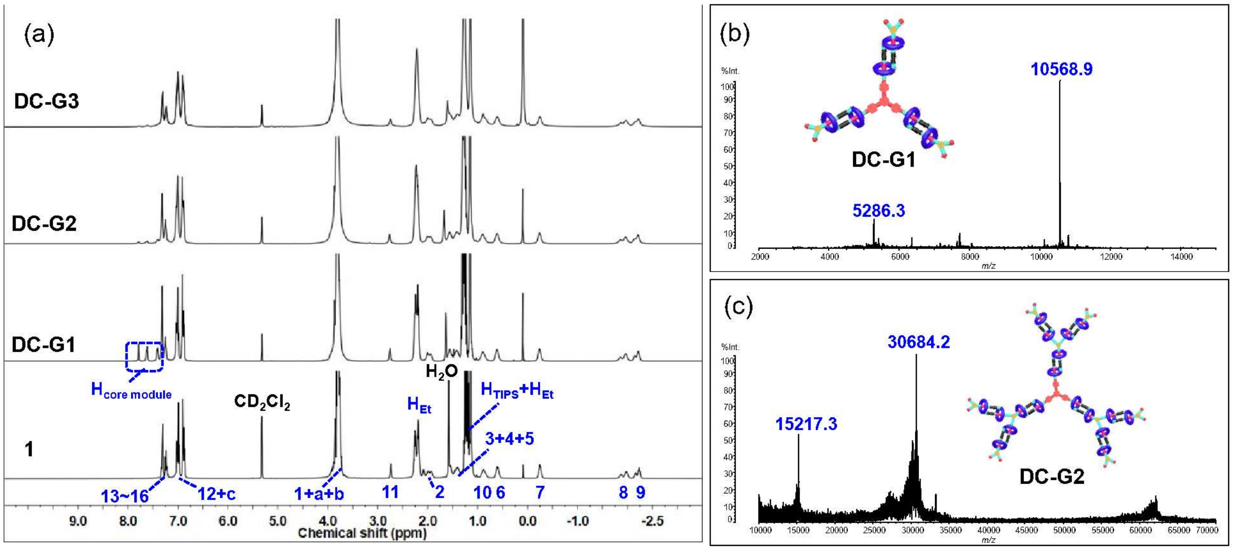

Figure 4. (a) Stacked ^{1}H NMR spectra of the [c2]daisy chain rotaxane **1** and daisy chain dendrimer **DC-G1**-**DC-G3**. MALDI-TOF-MS spectra of **DC-G1** (b) and **DC-G2** (c), respectively.

protected acetylene moieties in a yield of 84% yield. Following such iterative deprotection-coupling growth process, the third-generation daisy chain dendrimer **DC-G3** was successfully prepared with twenty-one individual [c2]daisy chain rotaxane units monodispersedly distributed in the dendrimer skeleton (Scheme S2-S4). Notably, the molecular weight of this daisy chain dendrimer is as high as 68,800 Da, which is even comparable with some proteins such as serum albumin.[20] In addition, the number of the [c2]daisy chain rotaxane units in it is almost twofold compared with the linear main chain poly[c2]daisy chain demonstrated by Stoddart et al..[13c] All of the above synthesized daisy chain dendrimers were soluble and stable in common organic solvents, thus making the purification process by means of column chromatography and preparative gel permeation chromatography (GPC) practical and scalable.

All the resultant daisy chain dendrimers were first characterized by 1-D NMR spectroscopy. In the ^{1}H NMR spectra, peaks attributed to mechanically interlocked structures, especially ones bellow 0.0 ppm, were observed, indicating that the [c2]daisy chain rotaxane units kept intact along with the dendrimer growth process. With the increase of the dendrimer generation, these signals became broader due to the slight in-equivalence of different generations (Figure 4a). In addition, as revealed by the ^{31}P NMR spectra, compared with the daisy chain dendrimers, the peak ascribed to the phosphine ligands of mono-substituted platinum-acetylide moiety in **1** displayed a remarkable downfield shift of ~2.7 ppm, which provided direct evidence to support the formation of platinum-acetylide bonds during the growth process of dendrimers as well as the integrity of the dendrimer skeleton (Figure S43). To confirm the successful synthesis of the targeted daisy chain dendrimers, the MALDI-TOF-MS measurements were performed. In the MALDI-TOF-MS spectrum of **DC-G1**, peaks of m/z =10,568.9 and m/z = 5,286.3 were observed, which fitted well with the theoretical values of [**DC-G1** + Na]$^+$ ion (m/z =10,570.0) and [**DC-G1** + H + Na]$^{2+}$ ion (m/z = 5,285.5), respectively (Figure 4b). For **DC-G2**, the peaks of m/z = 30,684.2 and m/z =15,217.3 were found in the MS spectrum, respectively, which could be attributed to the expected ion peaks with matrix molecules (Figure 4c). Unfortunately, even after continuous attempts, no satisfied MS data was obtained for **DC-G3** possibly due to its high molecular weight and low ionization efficiency. In order to confirm the formation of these large, monodispersed daisy chain dendrimers, GPC methodology was further performed, which revealed narrow distributions for the number-averaged molecular weight (M_n) with the polydispersity index (PDI) values of 1.02 (**DC-G1**), 1.02 (**DC-G2**) and 1.06 (**DC-G3**), respectively, thereby confirming the monodispersity of all daisy chain dendrimers (Figures S44-S46). More importantly, along with the increasing of the dendrimer generation, significant increase of the M_n values (for **DC-G1**, M_n = 8,754; for **DC-G2**, M_n = 25,151; for **DC-G3**, M_n = 52,873) was observed as well. Such expected trend provided indirect support for the successful synthesis of **DC-G3**.

In addition, UV-vis spectroscopy was employed to estimate the number of platinum-acetylide units in the daisy chain dendrimers, which provided further evidence for the successful synthesis of **DC-G3**. In the UV-vis spectra of the daisy chain dendrimers (Figure S53), two major absorption bands at around 293 and 346 nm were found, which were ascribed to the intra-ligand (IL) [π–π*(CR≡CR)] transitions and metal-to-ligand charge transfer (MLCT) [d(Pt)π–π*(CR≡CR)] transitions of platinum-acetylide units, respectively. Since the platinum-acetylide units in the resultant daisy chain dendrimers were well separated, no significant shifts of the $\lambda_{\max}$ values were observed. This observation indicated that there is no interaction between the inserted platinum-acetylide moieties. Thus the Lambert-Beer law ($A = \varepsilon lc$) can be used to determine the total number of platinum-acetylide units in the dendrimers. By comparing the molar extinction coefficient ε of the dendrimers listed in Table S1, we found that, for the absorption band at 346 nm attributed to the platinum-acetylide moieties, the ε value of **DC-G3** is about 7 times of that of **DC-G1**. According to the Lambert-Beer law, since six platinum-acetylide units (corresponding to three [c2]daisy chain rotaxane units) was confirmed in **DC-G1**, the number of the platinum-acetylide units in **DC-G3** was calculated to be 42, which indicated the existence of twenty-one [c2]daisy chain rotaxane units in **DC-G3**, thus confirming the successful synthesis of **DC-G3**.

With the targeted daisy chain dendrimers in hand, their morphologies were further investigated by using atomic force microscope (AFM), which revealed the discrete and uniform near-spherical morphologies for all daisy chain dendrimers (Figure 5). More importantly, along with the increase of the dendrimer generations, the averaged heights from AFM analysis gradually increased, from 3.9 ± 0.1 nm (**DC-G1**) to 8.9 ± 0.2 nm (**DC-G2**), and 12.8 ± 0.1 nm (**DC-G3**) respectively, which also provided a reasonable evidence for the successful construction of high-generation daisy chain dendrimers.

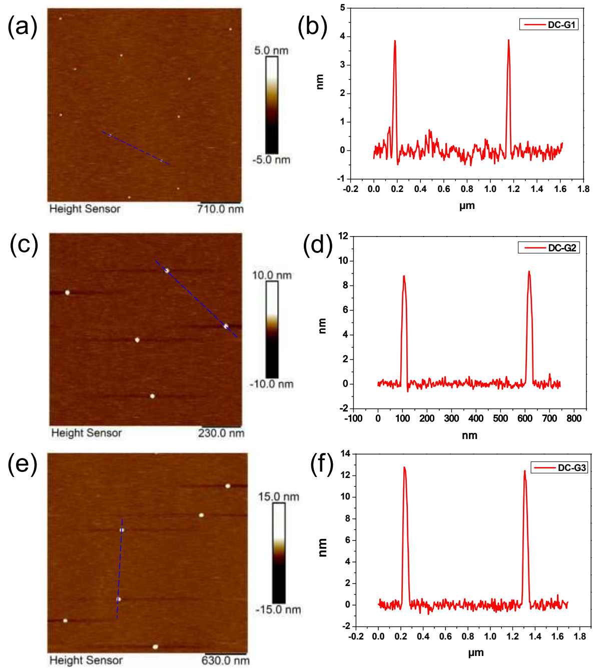

Figure 5. AFM images of daisy chain dendrimers. (a) **DC-G1**; (b) the height range of **DC-G1** is 3.9 ± 0.1 nm; (c) **DC-G2**; (d) the height range of **DC-G2** is 8.9 ± 0.2 nm; (e) **DC-G3**; (f) the height range of **DC-G3** is 12.8 ± 0.1 nm.

Dual stimuli-induced reversible dimension modulation of daisy chain dendrimers in solution state. Before evaluating the stimuli-induced dimension modulation feature of above synthesized daisy chain dendrimers, the investigation on the stimuli-responsiveness of the branches in the daisy chain dendrimers, *i.e.* the [c2]daisy chain rotaxane **2**, was first performed. According to the aforementioned design strategy, considering the binding ability as well as the availability for the reversible addition/removal of the external stimuli, acetate anion and DMSO solvent were chosen as the external stimulus, respectively. To our delight, as revealed by the ^{1}H NMR titration experiments, the continuous addition of tetrabutylammonium acetate (TBAA) into the solution of [c2]daisy chain rotaxane **2** in THF-d_8 resulted in the remarkable downfield shift of the signals of the protons that ascribed to the urea moieties (H_{11-12}) and the nearby methylene units (H_{8-10}). On the contrary, signals attributed to the neutral alkyl chain (H_{3-7}) displayed upfield shift simultaneously. These observations indicated that, upon the increase of amounts of the added acetate anions that can complex with urea moiety, the urea moieties as well as methylene units nearby moved out of the pillar[5]arene cavity, and the pillar[5]arene macrocycle moved towards the methylene units far away from the urea moieties. Furthermore, by subsequently adding $NaPF_6$ into the mixture of [c2]daisy chain rotaxane **2** and TBAA to completely remove the acetate anion as NaOAc precipitate, the resultant ^{1}H NMR spectrum was almost the same as the original one of [c2]daisy chain rotaxane **2**, confirming the reversibility of such stimuli-response extension/contraction process. As expected, when using DMSO molecule as stimulus, ^{1}H NMR titration experiments suggested the similar controllable and reversible muscle-like behavior of **2**, making **2** a dual stimuli-responsive artificial molecular muscle unit (Figures S55-S56). In order to gain more information on the cycle issue, the repetition of the translocation process of the [c2]daisy chain rotaxane unit **2** for 4 cycles was performed. As shown in Figures S57 and S58, respectively, for both acetate anions and DMSO molecules as stimuli, after each full operation cycle, the resultant ^{1}H NMR spectra were almost the same as the original one, thus indicating the good recycling ability of the [c2]daisy chain rotaxane unit. Such dual stimuli-responsive reversible and remarkable extension/contraction feature of **2** laid the foundation of the further dimension modulation of the integrated daisy chain dendrimers as discussed below. Notably, considering the integration of multiple [c2]daisy chain rotaxane units in a monodispersed manner within the skeletons, the amplified responsiveness of the daisy chain dendrimers towards the external stimulus might be possible.

To test such hypothesis, the stimuli-responsive behaviors of the daisy chain dendrimers were firstly investigated by ^{1}H NMR titration experiments (Figures S75-S83). To our delight, as same with the individual [c2]daisy chain rotaxane unit, all daisy chain dendrimers displayed the similar controllable and reversible dual stimuli-responsive features as indicated by the shifts of peaks that attributed to the [c2]daisy chain rotaxane units. Taking into consideration the remarkable length changes of these individual daisy chain units with external stimulus, investigations on the dimension modulation of the integrated daisy chain dendrimers upon the addition of acetate anion or DMSO molecule were then performed. As indicated by diffusion coefficients (*D*) of daisy chain dendrimers **DC-Gn** evaluated by 2-D diffusion-ordered spectroscopy (DOSY) technique, upon the addition of TBAA, remarkable increase of the diffusion coefficients (*D*) was observed (for **DC-G1**, from $(7.41 \pm 0.14) \times 10^{-10}$ m^2 s^{-1} to $(9.33 \pm 0.15) \times 10^{-10}$ m^2 s^{-1} with a shrinking ratio of 20%; for **DC-G2**, from $(3.31 \pm 0.12) \times 10^{-10}$ m^2 s^{-1} to $(4.27 \pm 0.10) \times 10^{-10}$ m^2 s^{-1} with a shrinking ratio of 22%, and for **DC-G3**, from $(3.98 \pm 0.06) \times 10^{-11}$ m^2 s^{-1} to $(5.89 \pm 0.05) \times 10^{-11}$ m^2 s^{-1} with a shrinking ratio of 32%, respectively), which clearly suggested the decrease of the hydrodynamic radius of daisy chain dendrimers. Subsequently, the addition of $NaPF_6$ into the resultant mixtures led to the decrease of diffusion coefficients to almost the original values, thus indicating the increase of the hydrodynamic radius back to their initial size (Figure 6b and Figures S84-S89). Furthermore, dynamic light scattering (DLS) experiments further provided the additional evidences for such anion-induced reversible dimensional modulation of **DC-Gn** in solution phase. The obvious decrease of the sizes of daisy chain dendrimers was observed after adding TBAA (for **DC-G1**, 3.8 ± 0.1 nm to 2.8 ± 0.2 nm with a shrinking ratio of 26%; for **DC-G2**, from 7.4 ± 0.1 nm to 5.1 ± 0.2 nm with a shrinking ratio of 30%; and for **DC-G3**, from 13.5 ± 0.2 nm to 7.2 ± 0.1 nm with a shrinking ratio of 46%, respectively). Furthermore, upon the removal of TBAA using $NaPF_6$, these sizes could almost recover back to their initial value (Figure 6c and Figures S99-S101), again confirming the reversibility of such dimension modulation process in solution phase. In the case of DMSO as stimulus, 2-D DOSY and DLS measurements revealed the similar reversible and controllable shrinking and swelling processes of daisy chain dendrimers upon the addition and removal of DMSO molecules with very approximate shrinking ratios with the case of acetate anion (Figures S102-S104 and Figure 6d). To confirm such dimension modulation process, small-angle neutron scattering (SANS), a powerful method to probe the structure with rich light atoms, especially hydrogen, was carried out in the solution phase. By doing Guinier analysis to the solution SANS data, the remarkable decrease of the radius of gyration (R_g) of the daisy chain dendrimer **DC-G3** upon the addition of external stimuli was observed. For instance, when acetate anions were added as stimulus, the R_g of **DC-G3** deceased from 7.64 nm to 6.91 nm, while in the case of DMSO molecules, from 8.12 nm to 7.22 nm, clearly suggesting the shrinking of the daisy chain dendrimer upon both stimuluses (Figure 6e).

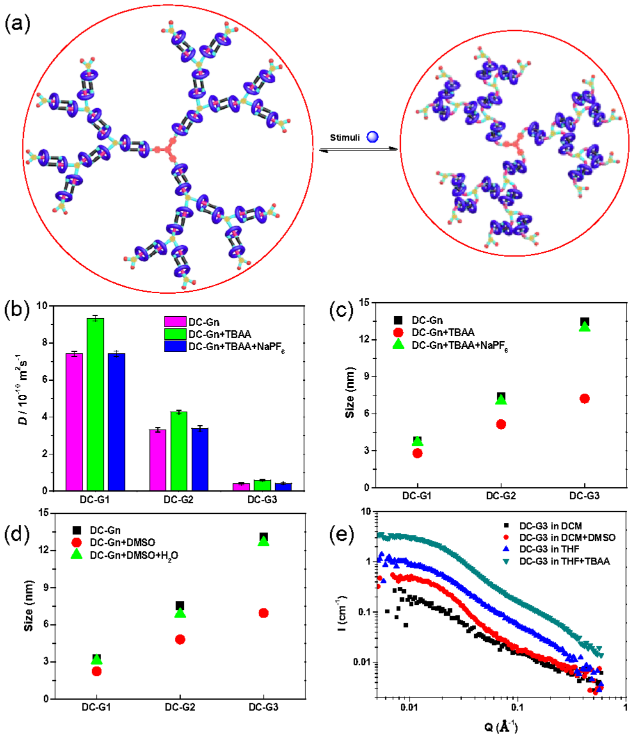

Figure 6. (a) Observed dimension modulation of daisy chain dendrimer **DC-G3** upon the addition of acetate anions or DMSO molecules as external stimuli in the solution state. (b) 2-D DOSY results of the anion-induced dimension modulation of daisy chain dendrimers **DC-Gn** (n = 1, 2, 3) in solution state. DLS resultants of the anion-induced (c) and solvent-induced (d) dimension modulation of daisy chain dendrimers **DC-Gn** (n = 1, 2, 3) in solution state, respectively. (e) SANS curves for the dual stimuli-induced dimension modulation of daisy chain dendrimer **DC-G3** in solution state.

In order to confirm such dimension modulation of the integrated daisy chain dendrimers was indeed attributed to the switchable molecular [2]daisy chain units, the model first-generation daisy chain dendrimer without urea moieties (**DC-G1-a**) was synthesized by employing the same controllable divergent approach from the corresponding model compound **1-a** (Scheme S5-S6). As expected, the addition of neither acetate anion nor DMSO-d_6 into the CD_2Cl_2 solution of **DC-G1-a** led to no changes in the resultant ^1H NMR spectra compared to the original one, which strongly suggested that the urea moieties did service as the binding site. More importantly, both 2-D DOSY and DLS measurements indicated the size of this model dendrimer remained unchanged before and after the addition of external stimulus (Figures S105-S116), which excluded the anion or solvent effect and confirmed that the swelling/shrinking of the daisy chain dendrimers originated from the collective muscle-like motions of individual [c2]daisy chain rotaxane branches.

According to above described controllable and reversible dimension modulation processes, it was possible that, in this study, besides the direct length change of individual [c2]daisy chain rotaxane moiety, the conformation changes, especially the self-folding, of these artificial molecular muscles might also contribute to the final outputs. In our case, the coordinative movements of two rigid P[5]A macrocycles to the center and the release of the flexible urea and alkyl moieties at the tails significantly decreased the rigidity of the [c2]daisy chain rotaxane units. Then, the [c2]daisy chain branches might efficiently adapt self-folding conformations in solution state that led to the shrinking of integrated daisy chain dendrimers (Figure 6a, Supplementary Movie S1). To confirm such hypothesis, geometry optimizations of **DC-G1** before and after the addition of acetate anion were performed by using the program MOPAC2016.[22] As revealed by the optimized structures shown in Figure S74, upon the addition of external stimulus, the remarkable contract of **DC-G1** was observed due to the remarkable self-folding of the three [c2]daisy chain branches.

Fast, reversible and controllable shape transformations of DC-Gn@PVDF composite films. After confirming the unique dimension modulation behavior of daisy chain dendrimers originated from the collective and amplified molecular motions of [c2]daisy chain rotaxane branches, we further employed daisy chain dendrimers for the construction of novel supramolecular dynamic materials. By the incorporation of daisy chain dendrimers into a polyvinylidene difluoride (PVDF) matrix, a series of composite polymer films **DC-Gn**@PVDF were successfully constructed via drop-spreading approach (for the details, see Section 7 in SI). In the resultant composite polymer films, the incorporated daisy chain dendrimers acted as stiff domains and their shrinking/swelling under external stimuli was expected to efficiently lead to controllable and reversible shape transformation behaviors of the resultant polymer materials.

To confirm such hypothesis, DMSO molecules were selected as the external stimulus. To our delight, all composite polymer films doped with the daisy chain dendrimers didn't display folding behaviors upon being immersed into water (State I, Figures 7a-c), while fast folding of the resultant composite polymer films was observed when DMSO was used as solvent (State II, Figures 7a-c). More interestingly, when keeping the mass fraction of daisy chain dendrimers at the same value of 35 wt%, for the higher-generation daisy chain dendrimers, a better folding capacity of the corresponding polymer films was revealed as indicated by the shorter time to reach the full-folding state (for **DC-G1**@PVDF, 148s; for **DC-G2**@PVDF, 114s; for **DC-G3**@PVDF, 39s) (Figures 7a-c and Supplementary Movies **DC-G1**-**DC-G3**). Considering almost the same [c2]daisy chain rotaxane density in all polymer films, an amplification effect of daisy chain dendrimers could be suggested, thus highlighting the superiority of the unique topological arrangements of molecular [c2]daisy chains within the dendrimer skeleton. When reducing the weigh fraction of daisy chain dendrimer to 10 wt% for **DC-G1**@PVDF, its folding capacity remained but with a slower self-folding speed (Figures S118), thus providing a practical method to tune the self-folding speed. For all cases, when re-immersing the fully folded films into water that can suck the DMSO molecules into the water phase, very fast de-folding phenomena within several seconds was observed (State I', Figures 7a-c), thus suggesting that DMSO molecules served as the stimulus to trigger such reversible and fast shape transformations of polymer films. Notably, such solvent-triggered reversible shape transformation process of the composite films could be repeated for at least 5 times without significant degradation in its performance (Figure S119). To further confirm the folding behavior of these polymer films originated from the stimuli-induced shrinking/swelling of the incorporated daisy chain dendrimers, the control experiments were performed. As shown in Figure S120, for the '*empty*' films (PVDF) and films with the model dendrimer **DC-G1-a** (**DC-G1-a**@PVDF) or the sole axle compound (**S_1**@PVDF), respectively, upon the sequential immerse into DMSO and water, no folding at all was observed in all cases, indicating the incorporated daisy chain dendrimers did take part in the folding process. On the basis of the aforementioned findings, the exact dimension modulation output of daisy chain dendrimers upon DMSO stimulus in the film state was then tested. To our delight, upon dropping DMSO solvent onto one side of the polymer films, the fast folding of the polymer films towards the other side was observed. After removing the DMSO by water washing, the recovery of film shapes to the original states was then achieved (Figure S121). Interestingly, such reversible folding/unfolding processes of the composite films could be also achieved by using DMSO/water vapor as triggers (Figure S122). Such controllable shape transformations of daisy chain dendrimers-based dynamic materials laid the foundation towards the construction of soft robotics that can perform programmed actions for practical uses.[23] Interestingly, from this intriguing controllable shape transformation phenomena, one could conclude that, along with the diffusion of DMSO molecules to one side of the films, the stimuli-induced motions of [c2]daisy chain rotaxane branches led to the swelling, rather than shrinking, of the integrated daisy chain dendrimers that further

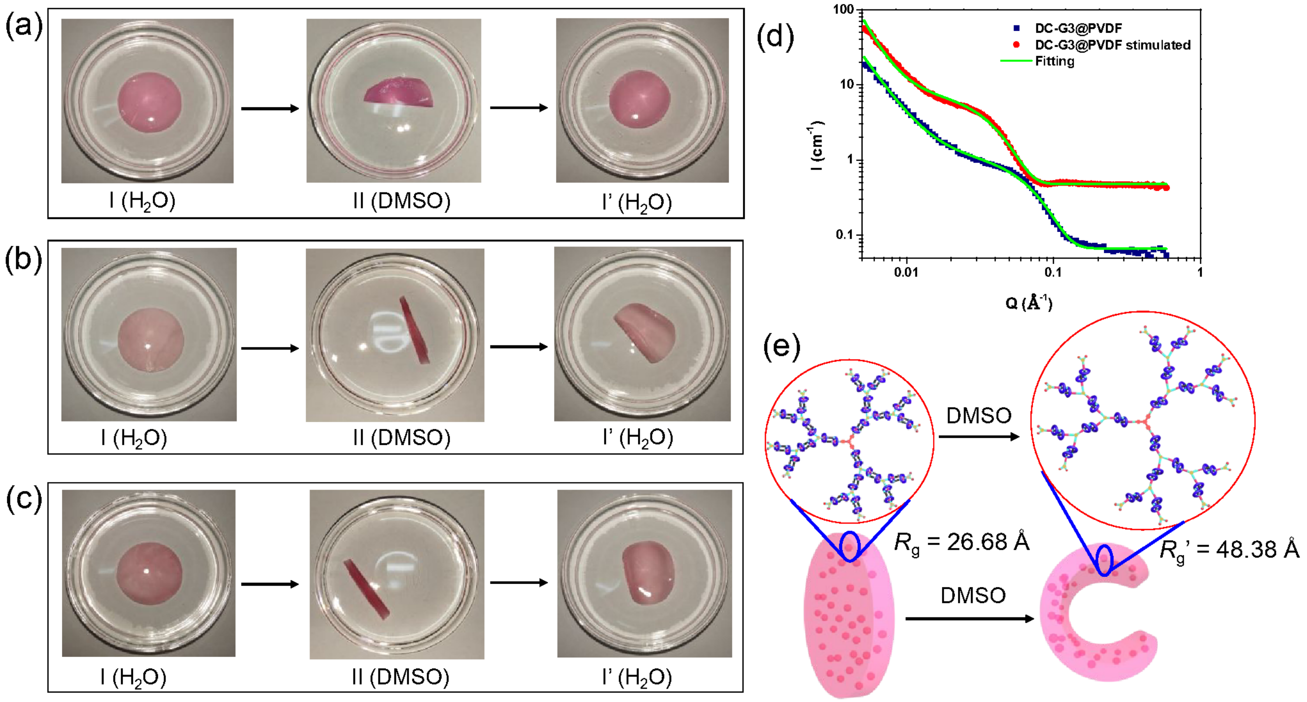

Figure 7. (a-c) Fast and reversible shape transformations of **DC-Gn**@PVDF (n = 1, 2, 3) films, respectively. (d) SANS curves for the solvent-induced dimension modulation of daisy chain dendrimer **DC-G3** in **DC-G3**@PVDF films. (e) Schematic illustration of the proposed mechanism of the controllable shape transformations of daisy chain dendrimer-based polymer composite films.

triggered the folding of the polymer films towards the opposite side (Figure 7e). Such actuating mechanism was confirmed by the SANS analysis of the polymer film as shown in Figure 7d. Using a Guinier function with a power law background to fit the SANS data, the R_g of the daisy chain dendrimer **DC-G3** before and after the addition of DMSO were evaluated, which revealed a remarkable increase from 2.67 nm to 4.84 nm, indicating the swelling of the incorporated daisy chain dendrimers that stimulated the shape transformation of the composite polymer film. Notably, the tunable dimension modulation outputs of daisy chain dendrimers in different states might be attributed to that, different from that in solution state, the polymer composites could efficiently inhibit the self-folding of [c2]daisy chain rotaxane branches in the film state, thus resulting in such state-dependent size switching feature of daisy chain dendrimers.

CONCLUSION

In this study, we proposed and successfully synthesized a new family of daisy chain dendrimers up to the third generation, in which twenty-one individual [c2]daisy chain rotaxanes served as branches monodisperesedly distributed within the dendrimer skeleton for the first time. In the resultant high-order MIMs, well-defined topological arrangement of multiple [c2]daisy chain rotaxanes was realized, thus allowing for the precise construction of a novel artificial molecular machine prototype. Interestingly, the controllable extension/contraction of individual [c2]daisy chain rotaxanes triggered by acetate anions or DMSO molecules as external stimuli led to stimuli-induced dimension modulation of the integrated daisy chain dendrimers through the collective and amplified motions of each branch. Moreover, the further incorporation of daisy chain dendrimers into a PVDF matrix resulted in the successful construction of the composite polymer films that could undergo fast, reversible and controllable shape transformations upon external stimulus. The demonstration of the stimuli-responsive daisy chain dendrimers with the tunable dimension modulation outputs herein provides a new strategy towards the construction of novel artificial molecular machine prototypes and supramolecular dynamic materials.

ASSOCIATED CONTENT

Supporting Information.

The Supporting Information is available free of charge on the ACS Publications website.

Additional information concerning the synthesis, characterization, and other experimental details.

AUTHOR INFORMATION

Corresponding Author

*hbyang@chem.ecnu.edu.cn (H.-B. Yang);
*weiwang@stu.ecnu.edu.cn (W. Wang);
*jin.wen@univie.ac.at (J. Wen);

ORCID

Jin Wen: 0000-0001-6136-8771
Hai-Bo Yang: 0000-0003-4926-1618

Notes

The authors declare no competing interest.

ACKNOWLEDGMENT

This work was financially supported by the NSFC/China (No. 21625202), Innovation Program of Shanghai Municipal Education Commission (No. 2019-01-07-00-05-E00012), and Program for Changjiang Scholars and Innovative Research Team in University for financial support. J. W. thanks to Austrian Science Fund (FWF): M 2709-N28. SANS measurements were performed at the Small Angle Neutron Scattering (SANS) instrument at China Spallation Neutron Source (CSNS). XANES measurements were performed at the BL15U1 beamline, Shanghai Synchrotron Radiation Source in China. We thank Prof. A. Dieter Schlüter (ETHZ) for his insightful comments and helpful discussions.

REFERENCES

(1) (a) Sluysmans, D.; Stoddart, J. F. The burgeoning of mechanically interlocked molecules in chemistry. *Trends in Chemistry* **2019**, *1*, 185-197. (b) Bruns, C. J.; Stoddart, J. F. The Nature of the Mechanical Bond (John Wiley & Sons, Hoboken, **2016**).

(2) (a) Erbas-Cakmak, S.; Leigh, D. A.; McTernan, C. T.; Nussbaumer, A. L. Artificial molecular machines. *Chem. Rev.* **2015**, *115*, 10081-10206. (b) Stoddart, J. F. Mechanically interlocked molecules (MIMs)—molecular shuttles, switches, and machines (Nobel Lecture). *Angew. Chem. Int. Ed.* **2017**, *56*, 11094-11125. (c) Sauvage, J.-P. From chemical topology to molecular machines (Nobel Lecture). *Angew. Chem. Int. Ed* **2017**, *56*, 11080-11093. (d) Zhang, L.; Marcos, V.; Leigh, D. A. Molecular machines with bio-inspired mechanisms. *Proc. Natl. Acad. Sci. USA*. **2018**. *115*, 9397-9404. (e) Wang, Q.; Chen, D.; Tian, H. Artificial molecular machines that can perform work. *Sci. China Chem.* **2018**, *61*, 1261-1273. (f) Heard, A. W.; Goldup, S. M. Simplicity in the design, operation, and applications of mechanically interlocked molecular machines. *ACS Cent. Sci.* **2020**, *6*, 117-128.

(3) (a) Anelli, P. L.; Spencer, N.; Stoddart, J. F. A molecular shuttle. *J. Am. Chem. Soc.* **1991**. *113*, 5131-5133. (b) Bissell, R. A.; Córdova, E.; Kaifer, A. E.; Stoddart, J. F. A chemically and electrochemically switchable molecular shuttle. *Nature* **1994**, *369*, 133-137. (c) Zhu, K.; O'Keefe, C.; Vukotic, V. N.; Schurko, R. W.; Loeb, S. J. A molecular shuttle that operates inside a metal-organic framework. *Nat. Chem.* **2015**, *7*, 514-519. (d) Zhu, K.; Baggi, G.; Loeb, S. J. Ring-through-ring molecular shuttling in a saturated [3]rotaxane. *Nat. Chem.* **2018**, *10*, 625-630. (e) Chen, S.; Wang, Y.; Nie, T.; Bao, C.; Wang, C.; Xu, T.; Lin, Q.; Qu, D.-H.; Gong, X.; Yang, Y.; Zhu, L.; Tian, H. An artificial molecular shuttle operates in lipid bilayers for ion transport. *J. Am. Chem. Soc.* **2018**, *140*, 17992-17998.

(4) (a) Lewandowski, B., De Bo, G., Ward, J. W., Papmeyer, M., Kuschel, S., Aldegunde, M. J., Gramlich, P. M. E., Heckmann, D., Goldup, S. M., D'Souza, D. M., Fernandes, A. E.; Leigh, D. A. Sequence-specific peptide synthesis by an artificial small-molecule machine. *Science* **2013**, *339*, 189-193. (b) De Bo, G.; Gall, M. A. Y.; Kitching, M. O.; Kuschel, S.; Leigh, D. A.; Tetlow, D. J.; Ward, J. W. Sequence-specific β-peptide synthesis by a rotaxane-based molecular machine. *J. Am. Chem. Soc.* **2017**, *139*, 10875-10879. (c) De Bo, G.; Gall, M. A. Y.; Kuschel, S.; De Winter, J.; Gerbaux, P.; Leigh, D. A. An artificial molecular machine that builds an asymmetric catalyst. *Nat. Nanotechnol.* **2018**, *13*, 381-385.

(5) (a) Cheng, C.; McGonigal, P. R.; Schneebeli, S. T.; Li, H.; Vermeulen, N. A.; Ke, C.; Stoddart, J. F. An artificial molecular pump. *Nat. Nanotechnol.* **2015**, 10, 547-553. (b) Meng, Z.; Xiang, J.-F.; Chen, C.-F. Directional molecular transportation based on a catalytic stopper-leaving rotaxane system. *J. Am. Chem. Soc.* **2016**, *138*, 5652- 5658. (c) Pezzato, C.; Nguyen, M. T.; Cheng, C.; Kim, D. J.; Otley, M. T.; Stoddart, J. F. An efficient artificial molecular pump.

Tetrahedron **2017**, *73*, 4849-4857. (d) Pezzato, C.; Nguyen, M. T.; Kim, D. J.; Anamimoghadam, O.; Mosca, L.; Stoddart, J. F. Controlling dual molecular pumps electrochemically. *Angew. Chem., Int. Ed.* **2018**, *57*, 9325-9329. (e) Qiu, Y.; Zhang, L.; Pezzato, C.; Feng, Y.; Li, W.; Nguyen, M. T.; Chen, C.; Shen, D.; Guo, Q.-H.; Shi, Y.; Cai, K.; Alsubaie, F. M.; Astumian, R. D.; Stoddart, J. F. A molecular dual pump. *J. Am. Chem. Soc.* **2019**, *141*, 17472-17476.

(6) (a) Leigh, D. A.; Wong, J. K. Y.; Dehez, F.; Zerbetto, F. Unidirectional rotation in a mechanically interlocked molecular rotor. *Nature* **2003**, *424*, 174-179. (b) Hernandez, J. V.; Kay, E. R.; Leigh, D. A. A reversible synthetic rotary molecular motor. *Science* **2004**, *306*, 1532- 1537. (c) Thordarson, P.; Bijsterveld, E. J. A.; Rowan, A. E.; Nolte, R. J. M. Epoxidation of polybutadiene by a topologically linked catalyst. *Nature* **2003**, *424*, 915-918. (d) Serreli, V.; Lee, C. F.; Kay, E. R.; Leigh, D. A. A molecular information ratchet. *Nature* **2007**, *445*, 523-527. Meng, Z.; Chen, C.-F. A molecular pulley based on a triply interlocked [2]rotaxane. *Chem. Commun.* **2015**, *51*, 8241-8244. (e) Erbas-Cakmak, S.; Fielden, S. D. P.; Karaca, U.; Leigh, D. A.; McTernan, C. T.; Tetlow, D. J.; Wilson, M. R. Rotary and linear molecular motors driven by pulses of a chemical fuel. *Science* **2017**, *358*, 340-343.

(7) (a) Gelles, J.; Schnapp, B. J.; Sheetz, M. P. Tracking kinesin-driven movements with nanometre-scale precision. *Nature* **1988**, *331*, 450-453. (b) Hirokawa, N.; Noda, Y.; Tanaka, Y.; Niwa, S. Kinesin superfamily motor proteins and intracellular transport. *Nat. Rev. Mol. Cell Biol.* **2009**, *10*, 682-696. (c) Hahn, S. Structure and mechanism of the RNA polymerase II transcription machinery. *Nat. Struct. Mol. Biol.* **2004**, *11*, 394-403. (d) RNA Polymerase as Molecular Motors (Buc, H. and Strick, T. Ed.) 1st ed., **2009**, Royal Society of Chemistry, Cambridge, UK. (e) Stock, D.; Leslie, A. G. W.; Walker, J. E. Molecular architecture of the rotary motor in ATP synthase. *Science* **1999**, *286*, 1700-1705. (f) Yoshida, M.; Muneyuki, E.; Hisabori, T. ATP synthase- a marvellous rotary engine of the cell. *Nat. Rev. Mol. Cell Biol.* **2001**, *2*, 669-677.

(8) (a) Ashton, P. R.; Baxter, I.; Cantrill, S. J.; Fyfe, M. C. T.; Glink, P. T.; Stoddart, J. F.; White, A. J. P.; Williams, D. J. Supramolecular daisy chains. *Angew. Chem. Int. Ed.* **1998**, *37*, 1294-1297. (b) Cantrill, S. J.; Youn, G. J.; Stoddart, J. F.; Williams, D. J. Supramolecular daisy chains. *J. Org. Chem.* **2001**, *66*, 6857-6872. (c) Rotzler, J.; Mayor, M. Molecular daisy chains. *Chem. Soc. Rev.* **2013**, *42*, 44–62. (d) Goujon, A.; Moulin, E.; Fuks, G.; Giuseppone, N. [c2]daisy chain rotaxanes as molecular muscles. *CCS Chemistry* **2019**, *1*, 83-96. (e) Fu, X; Zhang, Q.; Rao, S.-J.; Qu, D.-H.; Tian, H. One-pot synthesis of a [c2]daisy-chain-containing hetero[4]rotaxane via a self-sorting strategy. *Chem. Sci.* **2016**, *7*, 1696-1701. (f) Bruns, C. J.; Stoddart, J. F. Rotaxane-based molecular muscles. *Acc. Chem. Res.* **2014**, *47*, 2186-2199, and references therein.

(9) Cooke, R. The Sliding Filament Model: 1972–2004. *J. Gen. Physiol.* **2004**, *123*, 643-656.

(10) (a) Jiménez, M. C.; Dietrich-Buchecker, C.; Sauvage, J.-P. Towards synthetic molecular muscles: contraction and stretching of a linear rotaxane dimer. *Angew. Chem. Int. Ed.* **2000**, *39*, 3284-3287. (b) Collin, J.-P.; Dietrich-Buchecker, C.; Gaviña, P.; Jimenez-Molero, M. C.; Sauvage, J.-P., Shuttles and muscles: linear molecular machines based on transition metals. *Acc. Chem. Res.* **2001**, *34*, 477-487.

(11) (a) Wu, J.; Leung, K. C.-F.; Benítez, D.; Han, J.-Y.; Cantrill, S. J.; Fang, L.; Stoddart, J. F. An acid-base-controllable [c2]daisy chain. *Angew. Chem. Int. Ed.* **2008**, *47*, 7470-7474. (b) Coutrot, F.; Romuald, C.; Busseron, E. A new pH-switchable dimannosyl [c2]daisy chain molecular machine. *Org. Lett.* **2008**, *10*, 3741-3744. (c) Zhang, Z.; Han, C.; Yu, G.; Huang, F. A solvent-driven molecular spring. *Chem. Sci.* **2012**, *3*, 3026-3031. (d) Weigandt, J.; Chung, C.-L.; Jester, S.-S.; Famulok, M. Daisy chain rotaxanes made from interlocked DNA nanostructures. *Angew. Chem. Int. Ed.* **2016**, *55*, 5512–5516. (e) Chang, J.-C.; Tseng, S.-H.; Lai, C.-C.; Liu, Y.-H.; Peng, S.-M.; Chiu, S.-H. Mechanically interlocked daisy-chain-like structures as multidimensional molecular muscles. *Nat. Chem.* **2017**, *9*, 128-134. (f) Zhang, Q.; Rao, S.-J.; Xie, T.; Li, X.; Xu, T.-Y.; Li, D.-W.; Qu, D.-H.; Long, Y.-T.; Tian, H. Muscle-like artificial molecular actuators for nanoparticles. *Chem* **2018**, *4*, 2670-2684.

(12) Krans, J. L. The sliding filament theory of muscle contraction. *Nat. Educ.* **2010**, *3*, 66.

(13) (a) Guidry, E. N.; Li, J.; Stoddart, J. F.; Grubbs, R. H. Bifunctional [c2]daisy-chains and their incorporation into mechanically interlocked polymers. *J. Am. Chem. Soc.* **2007**, *129*, 8944-8945. (b) Clark, P. G.; Day, M. W.; Grubbs, R. H. Switching and extension of a [c2]daisy-chain dimer polymer. *J. Am. Chem. Soc.* **2009**, *131*, 13631-13633. (c) Fang, L.; Hmadeh, M.; Wu, J.; Olson, M. A.; Spruell, J. M.; Trabolsi, A.; Yang, Y.-W.; Elhabiri, M.; Albrecht-Gary, A.-M.; Stoddart, J. F. Acid−base actuation of [c2]daisy chains. *J. Am. Chem. Soc.* **2009**, *131*, 7126-7134. (d) Hmadeh, M.; Fang, L.; Trabolsi, A.; Elhabiri, M.; Albrecht-Gary, A.-M.; Stoddart, J. F. On the thermodynamic and kinetic investigations of a [c2]daisy chain polymer. *J. Mater. Chem.* **2010**, *20*, 3422-3430.

(14) (a) Du, G.; Moulin, E.; Jouault, N.; Buhler, E.; Giuseppone, N. Muscle-like supramolecular polymers-integrated motions from thousands of molecular machines. *Angew. Chem. Int. Ed.* **2012**, *51*, 12504-12508. (b) Goujon, A.; Du, G.; Moulin, E.; Fuks, G.; Maaloum, M.; Buhler, E.; Giuseppone, N. Hierarchical self-assembly of supramolecular muscle-like fibers. *Angew. Chem. Int. Ed.* **2016**, *55*, 703-707. (c) Goujon, A.; Mariani, G.; Lang, T.; Moulin, E.; Rawiso, M.; Buhler, E.; Giuseppone, N. Controlled sol-gel transitions by actuating molecular machine based supramolecular polymers. *J. Am. Chem. Soc.* **2017**, *139*, 4923-4928. (d) Gao, L.; Zhang, Z.; Zheng, B.; Huang, F. Construction of muscle-like metallo-supramolecular polymers from a pillar[5]arene-based [c2]daisy chain. *Polym. Chem.* **2014**, *5*, 5734–5739. (e) Fu, X.; Gu, R.-R.; Zhang, Q.; Rao, S.-J.; Zheng, X.-L.; Qu, D.-H.; Tian, H. Phototriggered supramolecular polymerization of a [c2]daisy chain rotaxane. *Polym. Chem.* **2016**, *7*, 2166-2170.

(15) (a) Iwaso, K.; Takashima, Y.; Harada, A. Fast response dry-type artificial molecular muscles with [c2]daisy chains. *Nat. Chem.* **2016**, *8*, 625-632. (b) Ikejiri, S.; Takashima, Y.; Osaki, M.; Yamaguchi, H.; Harada, A. Solvent-free photoresponsive artificial muscles rapidly driven by molecular machines. *J. Am. Chem. Soc.* **2018**, *140*, 17308-17315.

(16) (a) Coskun, A.; Banaszak, M.; Astumian, R. D.; Stoddart, J. F.; Grzybowski, B. A. Great expectations: can artificial molecular machines deliver on their promise? *Chem. Soc. Rev.* **2012**, *41*, 19-30. (b) Kim, S.-Y.; Ko, Y. H.; Lee, J. W.; Sakamoto, S.; Yamaguchi, K.; Kim, K. Toward high-generation rotaxane dendrimers that incorporate a ring component on every branch: noncovalent synthesis of a dendritic [10]pseudorotaxane with 13 molecular components. *Chem. - Asian J.* **2007**, *2*, 747-754. (c) Kwan, C.-S.; Zhao, R.; Van Hove, M. A.; Cai, Z.; Leung, K. C.-F. Higher-generation type III-B rotaxane dendrimers with controlling particle size in three-dimensional molecular switching. *Nat. Commun.* **2018**, *9*, 497. (d) Wang, W.; Chen, L.-J.; Wang, X.-Q.; Sun, B.; Li, X.; Zhang, Y.; Shi, J.; Yu, Y.; Zhang, L.; Liu, M.; Yang, H.-B. Organometallic rotaxane dendrimers with fourth-generation mechanically interlocked branches. *Proc. Natl. Acad. Sci. USA.* **2015**, *112*, 5597-5601. (e) Wang, X.-Q.; Wang, W.; Li, W.-J.; Chen, L.-J.; Yao, R.; Yin, G.-Q.; Wang, Y.-X.; Zhang, Y.; Huang, J.; Tan, H.; Yu, Y.; Li, X.; Xu, L.; Yang, H.-B. Dual stimuli-responsive rotaxane-branched dendrimers with reversible dimension modulation. *Nat. Commun.* **2018**, *9*, 3190. (f) Wang, X.-Q.; Li, W.-J.; Wang, W.; Wen, J.; Zhang, Y.; Tan, H.; Yang, H.-B. Construction of Type III-C rotaxane-branched dendrimers and their anion-induced dimension modulation feature. *J. Am. Chem. Soc.* **2019**, *141*, 13923-13930. (g) Yan, X.; Zheng, B.; Huang, F. Integrated motion of molecular machines in supramolecular polymeric scaffolds. *Polym. Chem.* **2013**, *4*, 2395-2399. (h) Bruns, C. J.; Stoddart, J. F. Molecular machines muscle up. *Nat. Nanotechnol.* **2013**, *8*, 9-10. (i) Lu, Y.; Lin, Y.; Li, Z.; Jin, G. Highly stable molecular borromean rings, *Chin. J. Chem.* **2018**, *36*, 106-111.

(17) (a) Vögtle, F.; Richardt, G.; Werber, N. Dendrimer Chemistry: Concepts, Syntheses, Properties, Applications; Wiley: Weinheim,

2009. (b) Xu, L.; Chen, L.-J.; Yang, H.-B. Recent progress in the construction of cavity-cored supramolecular metallodendrimers via coordina-tion-driven self-assembly. *Chem. Commun.* **2014**, *50*, 5156-5170. (c) Chen, L.-J.; Zhao, G.-Z.; Jiang, B.; Sun, B.; Wang, M.; Xu, L.; He, J.; Abliz, Z.; Tan, H.; Li, X.; Yang, H.-B. Smart stimuli-responsive spherical nanostructures constructed from supramolecular metal-lodendrimers via hierarchical self-assembly. *J. Am. Chem. Soc.* **2014**, *136*, 5993-6001. (d) Lee, J. K.; Kim, K. Rotaxane dendrimers. *Top. Curr. Chem.* **2003**, *228*, 111-140. (e) Leung, K. C.-F.; Lau, K. N. Self-assembly and thermodynamic synthesis of rotaxane dendrimers and related structures. *Poly. Chem.* **2010**, *1*, 988-1000. (f) Chen, C.-F. High-generation organometallic rotaxane dendrimer. *Sci. China Chem.* **2015**, *58*, 1089.

(18) (a) Ogoshi, T.; Kanai, S.; Fujinami, S.; Yamagishi, T.; Nakamoto, Y. para-Bridged symmetrical pillar[5]arenes: their Lewis acid catalyzed synthesis and host-guest property. *J. Am. Chem. Soc.* **2008**, *130*, 5022-5023. (b) Xue, M.; Yang, Y.; Chi, X.; Zhang, Z.; Huang, F. Pillararenes, a new class of macrocycles for supramolecular chemistry. *Acc. Chem. Res.* **2012**, *45*, 1294-1308. (c) Ogoshi, T.; Yamagishi, T.-a.; Nakamoto, Y. Pillar-shaped macrocyclic hosts pillar[n]arenes: new key players for supramolecular chemistry. *Chem. Rev.* **2016**, *116*, 7937-8002. (d) Jiang, B.; Wang, W.; Zhang, Y.; Lu, Y.; Zhang, C.-W.; Yin, G.-Q.; Zhao, X.-L.; Xu, L.; Tan, H.; Li, X.; Jin, G.-X.; Yang, H.-B. Construction of π-surface-metalated pillar[5]arenes which bind anions via anion–π interactions. *Angew. Chem. Int. Ed.* **2017**, *56*, 14438-14442. (e) Jie, K.; Zhou, Y.; Li, E.; Huang, F. Nonporous adaptive crystals of pillararenes. *Acc. Chem. Res.* **2018**, *51*, 2064-2072. (f) Kakuta, T.; Yamagishi, T.-a.; Ogoshi, T. Stimuli-responsive supramolecular assemblies constructed from pillar[n]arenes. *Acc. Chem. Res.* **2018**, *51*, 1656-1666. (g) Song, N.; Kakuta, T.; Yamagishi, T.; Yang, Y.-W.; Ogoshi, T. Molecular-scale porous materials based on pillar[n]arenes. *Chem* **2018**, *4*, 2029-2053. (h) Fa, S.; Kakuta, T.; Yamagishi, T.-a.; Ogoshi, T. One-, two-, and three-dimensional supramolecular assemblies based on tubular and regular polygonal structures of pillar[n]arenes. *CCS Chemistry* **2019**, *1*, 50-63.

(19) (a) Leininger, S.; Stang, P. J.; Huang, S. Synthesis and characterization of organoplatinum dendrimers with 1,3,5-triethynylbenzene building blocks. *Organometallics* **1998**, *17*, 3981-3987. (b) Wang, W.; Yang, H.-B.; Linear neutral platinum–acetylide moiety: beyond the links. *Chem. Commun.* **2014**, *50*, 5171-5186. (c) Jiang, B.; Zhang, J.; Ma, J.-Q.; Zheng, W.; Chen, L.-J.; Sun, B.; Li, C.; Hu, B.-W.; Tan, H.; Li, X.; Yang, H.-B. Vapochromic behavior of a chair-shaped supramolecular metallacycle with ultra-stability. *J. Am. Chem. Soc.* **2016**, *138*, 738-741. (d) Xu, L.; Yang, H.-B. Our expedition in linear neutral platinum-acetylide complexes: the preparation of micro/nanostructure materials, complicated topologies, and dye-sensitized solar cells. *Chem. Rec.* **2016**, *16*, 1274-1297. (e) Chen, L.-J.; Yang, H.-B. Construction of stimuli-responsive functional materials via hierarchical self-assembly involving coordination interactions. *Acc. Chem. Res.* **2018**, *51*, 2699-2710. (f) Wong, K. M.-C.; Yam, V. W.-W. Self-assembly of luminescent alkynylplatinum (II) terpyridyl complexes: Modulation of photophysical properties through aggregation behavior. *Acc. Chem. Res.* **2011**, *44*, 424-434. (g) Yam, V. W.-W.; Au, V. K.-M. S.; Leung, Y.-L. Light-emitting self-assembled materials based on d^8 and d^{10} transition metal complexes. *Chem. Rev.* **2015**, *115*, 7589-7728. (h) Chan, A. K.-W.; Yam, V. W.-W. Precise modulation of molecular building blocks from tweezers to rectangles for recognition and stimuli-responsive processes. *Acc. Chem. Res.* **2018**, *51*, 3041-3051. (i) Zheng, W.; Wang, W.; Jiang, S.-T.; Yang, G.; Li, Z.; Wang, X.-Q.; Yin, G.-Q.; Zhang, Y.; Tan, H.; Li, X.; Ding, H.; Chen, G.; Yang, H.-B. Supramolecular transformation of metallacycle-linked star polymers driven by simple phosphine ligand-exchange reaction. *J. Am. Chem. Soc.* **2019**, *141*, 583-591. (j) Wang, Y.-X.; Zhou, Q.-F.; Chen, L.-J.; Xu, L.; Wang, C.-H.; Li, X.; Yang, H.-B. Facile construction of organometallic rotaxane-terminated dendrimers using neutral platinum–acetylides as the main scaffold. *Chem. Commun.* **2018**, *54*, 2224-2227. (k) Wang, X.-Q.; Wang, W.; Li, W.-J.; Qin, Y.; Yin, G.-Q.; Jiang, W.-L.; Li, X.; Wu, S.; Yang, H.-B. Rotaxane-branched dendrimers with aggregation-induced emission behavior. *Org. Chem. Front.* **2019**, *6*, 1686-1691. (l) He, M.; Chen, L.; Jiang, B.; Tan, H.; Wang, C.; Yang, H. Facile construction of Zn(II)-porphyrin-cored [5]rotaxane and its controllable aggregation behaviours. *Chin. Chem. Lett.* **2019**, *30*, 131-134. (m) Chen, Z.; Chan, A. K.-W.; Wong, V. C.-H.; Yam, V. W.-W. A supramolecular strategy toward an efficient and selective capture of platinum(II) complexes. *J. Am. Chem. Soc.* **2019**, *141*, 11204-11211. (n) Chan, C. K. M.; Tao, C.-H.; Tam, H.-L.; Zhu, N.; Yam, V. W.-W.; Cheah, K.-W. Synthesis, characterization, luminescence, and non-linear optical properties of oxadiazole- and truxene-containing platinum(II) alkynyl complexes with donor-acceptor functionalities. *Inorg. Chem.* **2009**, *48*, 2855-2864. (o) Ohshiro, N.; Takei, F.; Onitsuka, K.; Takahashi, S. Synthesis of organometallic dendrimers with a backbone composed of platinum-acetylide units. *J. Organomet. Chem.* **1998**, *569*, 195-202. (p) Onitsuka, K.; Fujimoto, M.; Ohshiro, N.; Takahashi, S. Convergent route to organometallic dendrimers composed of platinum-acetylide units. *Angew. Chem. Int. Ed.* **1999**, *38*, 689-692. (q) Onitsuka, K.; Fujimoto, M.; Kitajima, H.; Ohshiro, N.; Takei, F. Takahashi, S. Convergent synthesis of platinum-acetylide dendrimers, *Chem. Eur. J.* **2004**, *10*, 6433-6446. (r) Chen, L.-J.; Zhang, J.; He, J.; Xu, X.-D.; Wu, N.-W.; Wang, D.-X.; Abliz, Z.; Yang, H.-B. Synthesis of platinum acetylide derivatives with different shapes and their gel formation behavior, *Organometallics* **2011**, *30*, 5590-5594.

(20) Hirayama, K.; Akashi, S.; Furuya, M.; Fukuhara, K. L. Rapid confirmation and revision of the primary structure of bovine serum albumin by ESIMS and Frit-FAB LC/MS. *Biochem. Biophys. Res. Commun.* **1990**, *173*, 639-646.

(21) Ornelas, C.; Ruiz, J.; Belin, C.; Astruc, D. Giant dendritic molecular electrochrome batteries with ferrocenyl and pentamethylferrocenyl termini. *J. Am. Chem. Soc.* **2009**, *131*, 590-601. Notably, in the UV-vis analysis of the daisy chain dendrimers, in order to exclude the aggregation of the daisy chain dendrimer molecules that might perturb the validity of the Lambert-Beer law, highly dilute solutions ($c = 10^{-6}$ M) were used.

(22) Stewart, J. J. P. Stewart Computational Chemistry-MOPAC (Colorado Springs, CO, USA, **2016**).

(23) Whitesides, G. M. Soft robotics. *Angew. Chem. Int. Ed.* **2018**, *57*, 4258-4273.

Table of Contents